remote sensing

MDPI

Communication

Joint Wideband Beamforming Algorithm for Main Lobe Jamming Suppression in Distributed Array Radar

Xiaofeng Ma, Siqin Jiang, Shurui Zhang *, Renli Zhang and Weixing Sheng

School of Electronic and Optical Engineering, Nanjing University of Science and Technology, Nanjing 210094, China; zhangrenli@njust.edu.cn (R.Z.); shengwx@njust.edu.cn (W.S.)
* Correspondence: shuruizhang@njust.edu.cn

Abstract: In the increasingly complex electromagnetic environment, main lobe jamming significantly degrades the performance of a wideband radar system. To mitigate this issue, this paper developed a wideband main lobe jamming suppression algorithm based on a distributed array radar. Firstly, this algorithm utilizes eigen-projection matrix processing in the main array to cancel out the main lobe jamming for main lobe maintenance, and then suppresses side lobe jamming through null constraint beamforming. Subsequently, the large aperture of the full array is leveraged to form a narrow beam directed toward the main lobe interference. Finally, joint beamforming using the minimum mean square error criterion is employed. In scenarios where both main lobe jamming and side lobe jamming exist, this algorithm can adaptively cancel main lobe wideband jamming, suppress side lobe wideband jamming, and effectively control the significant loss of the desired wideband signals caused by main lobe jamming within a smaller angular range. Simulation results validate the effectiveness of the algorithm.

Keywords: distributed wideband array radar; main lobe jamming suppression; eigen-projection matrix processing (EMP); minimum mean square error (MMSE)

Citation: Ma, X.; Jiang, S.; Zhang, S.; Zhang, R.; Sheng, W. Joint Wideband Beamforming Algorithm for Main Lobe Jamming Suppression in Distributed Array Radar. *Remote Sens.* **2024**, *16*, 2402. https://doi.org/10.3390/rs16132402

Academic Editor: Piotr Samczynski

Received: 6 June 2024
Revised: 26 June 2024
Accepted: 29 June 2024
Published: 30 June 2024

1. Introduction

As radar technology continues to evolve and innovate, radar systems have become indispensable technological equipment in modern society. However, in the actual application process, radar is often affected by various types of jamming, among which main lobe jamming is a common and serious form [1,2]. Main lobe jamming refers to external signal jamming from the main lobe direction of the radar system. Such jamming can lead to radar system errors in target position determination, weakened target detection ability, reduced tracking accuracy, and significant impacts on the performance and reliability of the radar system [3–5]. Thus, it is crucial to enhance the anti-jamming capability of the radar system's adaptive array.

To effectively address main lobe jamming, numerous anti-jamming methods and techniques have been proposed. Adaptive beamforming technology stands out as a commonly employed approach [6]. It utilizes signal information received by the array antenna to dynamically adjust beam direction and gain, minimizing jamming signals. However, when used alone to counter main lobe jamming, this technique can result in main lobe distortion, impacting target detection capabilities [7].

Traditional single-radar array systems are inadequate for coping with the growing complexity of main lobe jamming. In response to this challenge, MIMO [8] and distributed radar technology have emerged. Distributed array radar [9,10] deploys multiple small, mobile radars in various locations, enhancing the system's anti-jamming capability and survivability through information fusion and cooperative operations, making it a focal point in current radar technology development. An interferometric array with the same size as the main array and two antenna arrays positioned far apart is introduced [11]. However,

this method only marginally reduces desired signal loss, with effectiveness decreasing as the array size increases. A main lobe jamming suppression technique based on a large aperture auxiliary array is proposed in [12], which allows for complete retention of the main lobe. On this basis, a wideband distributed array radar method based on whitening filters is proposed to suppress the main lobe jamming [13]. However, the computational complexity of the method is also significantly amplified due to the large auxiliary array. In [14], a sparse distributed phased MIMO radar algorithm with high angular resolution is proposed. The concurrent high sidelobe problem is solved by optimizing the subarray layout and receiving weighting coefficients under practical constraints. A joint jamming cancellation scheme based on sub-band processors is proposed to enhance jamming cancellation in wideband digital array radar systems [15].

In practice, the jamming environment often presents multiple sources of jamming, increasing its complexity. While distributed array radars offer anti-jamming capabilities, these capabilities are limited by the degrees of freedom, which are directly tied to the number of auxiliary arrays. However, in real-world applications, expanding the number of auxiliary arrays is often constrained by cost considerations. To address this challenge, an adaptive–adaptive joint beamforming method is proposed to simultaneously suppress main and side lobe jamming [16]. When the apertures of the primary and auxiliary arrays differ, residual jamming may occur. To mitigate this issue, a joint beamforming method based on feature projection preprocessing and zero constraints is suggested [17]. However, it is worth noting that the aforementioned methods are primarily applicable to narrowband signals. Research on wideband distributed array radar main lobe jamming suppression methods is relatively limited.

In this paper, a novel distributed array radar method is proposed to suppress wideband main lobe jamming. Firstly, a brief overview of the principles of distributed wideband radar and establishes the corresponding signal model is presented. Furthermore, the proposed wideband main lobe jamming suppression algorithm based on distributed radar, including main array, full array beamforming, and joint beamforming using minimum mean square error (MMSE), is presented in detail. Simulation results show that the proposed algorithm is correct and effective.

2. Wideband Distributed Array Radar Signal Model

Distributed array radar is a new system of radar that can receive signals in all directions, angles, and dimensions, thereby detecting target information more accurately than a single radar. The system consists of a main radar and multiple auxiliary radars, which are deployed at specific locations and work in concert to form an equivalent large aperture distributed array. In the presence of main lobe jamming, such array characteristics are commonly exploited to transfer the main lobe jamming of the main array to the sidelobe of the distributed array, utilizing the extremely high angle resolution of the full array to counteract the main lobe jamming of the main radar [18]. These radar arrays can be flexibly selected and combined to form various apertures to suit different missions and environmental requirements.

The algorithm proposed in this paper considers two sets of apertures—the main radar array and the full array of distributed array radars. The large aperture of the full array provides high angular resolution, enabling it to form narrow beams directed towards the main lobe jamming. Assuming there are $N + 1$ arrays arranged in the form of a one-dimensional linear array, where N is the total number of auxiliary radars, and each array has M elements, as depicted in Figure 1. Meanwhile, the main and auxiliary arrays are assumed to be half-wavelength uniform linear arrays. To facilitate the analysis, the distributed array radar can be regarded as a sparse array with $N + 1$ array elements.

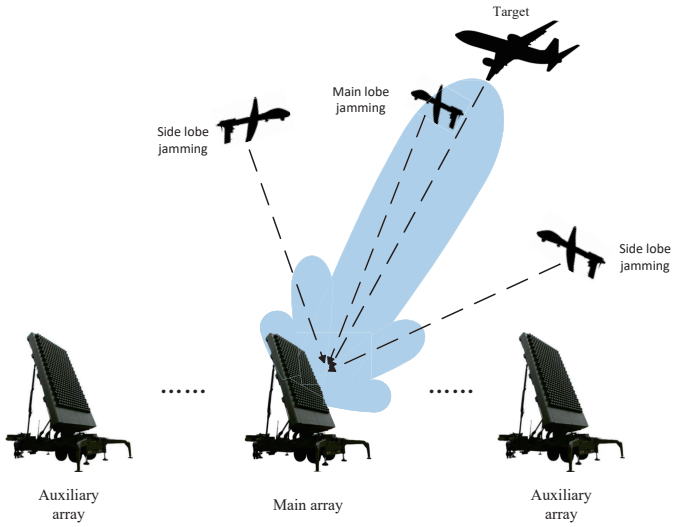

Figure 1. Schematic diagram of the distributed array radar.

Consider that there are p interfering signals with an incidence direction of θ_i $(i = 1, 2, \cdots, p)$ and an expected signal with an incidence direction of θ_0 shot at the array, with independently uncorrelated Gaussian white noise between each array element. In this case, the received signal of the array can be formulated as

$$\mathbf{x}(t) = \mathbf{a}(\theta_0, f)\mathbf{s}_0(t) + \sum_{i=1}^{p} \mathbf{a}(\theta_i, f)\mathbf{s}_i(t) + \mathbf{n}(t) \tag{1}$$

where $\mathbf{s}_0(t)$ and $\mathbf{s}_i(t)$ are the complex envelopes of the desired signal and the ith interfering signal, respectively, $\mathbf{a}(\theta_0, f)$ and $\mathbf{a}(\theta_i, f)$ are the steering vectors of the corresponding signals in the subsequent format, and $\mathbf{n}(t)$ is the received noise,

$$\mathbf{a}(\theta, f) = [e^{\frac{j2\pi d_0 f \sin(\theta)}{c}}, \cdots, e^{\frac{j2\pi d_i f \sin(\theta)}{c}}, \cdots, e^{\frac{j2\pi d_N f \sin(\theta)}{c}}]^T \tag{2}$$

where d_i denotes the distance between the ith radar array and the array phase center, c represents the speed of electromagnetic propagation. In this context, the phase center of the first auxiliary array is regarded as the phase center of the full array.

The received signal is decomposed into J sub-bands by discrete Fourier transform, then the signal in the sub-band with center frequency f_j can be expressed as follows.

$$\mathbf{X}(f_j) = \mathbf{A}(f_j)\mathbf{S}(f_j) + \mathbf{N}(f_j) \tag{3}$$

3. Wideband Main Lobe Jamming Suppression Algorithm

In this section, we detail the proposed method for suppressing main lobe jamming, depicted schematically in Figure 2. As illustrated, the method consists of three main parts. Firstly, employing the eigen-projection matrix processing (EMP) algorithm and null constraint beamforming in the main array to achieve side lobe jamming suppression with main lobe preservation. Secondly, the main lobe jamming angle is obtained through spatial spectrum estimation, followed by the formation of a narrow beam pointing towards the main beam jamming within the full array. Finally, we combine the beamforming outputs from both the main array and the full array, leveraging MMSE criterion for joint beamforming to effectively suppress main lobe jamming.

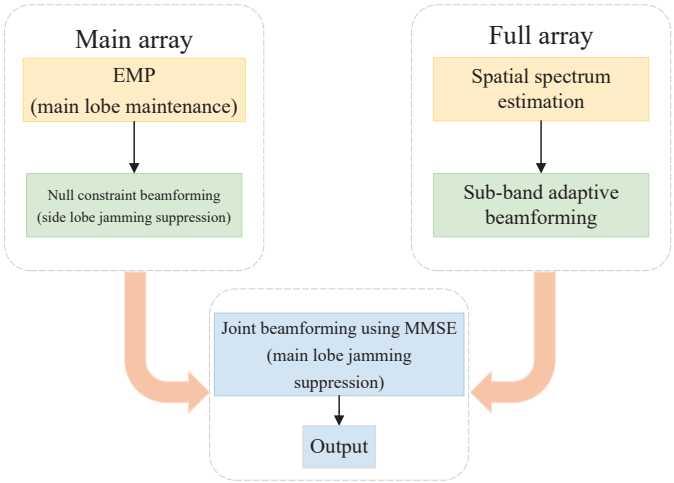

Figure 2. Block diagram of the proposed algorithm.

3.1. Beamforming for Single Wideband Array

The algorithm utilized in the main array is elucidated below, taking the j-th sub-band as an example. In the event that there are p jammings, including just one main lobe jamming, the eigenvalue decomposition of the covariance matrix $\mathbf{R}_{main}(f_j)$, which encompasses solely jamming and noise in the main array, is denoted as

$$\mathbf{R}_{main}(f_j) = \sum_{i=1}^{M} \lambda_i \mathbf{u}_i \mathbf{u}_i^H = \mathbf{U}_s \mathbf{\Lambda}_s \mathbf{U}_s^H + \mathbf{U}_n \mathbf{\Lambda}_n \mathbf{U}_n^H \tag{4}$$

where $\lambda_i (i = 1, 2, \cdots, M)$ is the eigenvalue of the covariance matrix $\mathbf{R}_{main}(f_j)$ and $\lambda_1 \geq \lambda_2 \geq \cdots \geq \lambda_{p-1} \geq \lambda_p \geq \cdots \geq \lambda_M$, $\mathbf{u}_i$ are the eigenvectors corresponding to the eigenvalue λ_i. $\mathbf{u}_1, \mathbf{u}_2, \cdots, \mathbf{u}_p$ are tensed into the jamming subspace $\mathbf{U}_s$, and $\mathbf{u}_{p+1}, \mathbf{u}_{p+2}, \cdots, \mathbf{u}_M$ are tensed into the noise subspace $\mathbf{U}_n$,

$$\begin{aligned} \mathbf{U}_s &= [\mathbf{u}_1, \mathbf{u}_2, \cdots, \mathbf{u}_p] \\ \mathbf{\Lambda}_s &= \mathrm{diag}(\lambda_1, \lambda_2, \cdots, \lambda_p) \\ \mathbf{U}_n &= [\mathbf{u}_{p+1}, \mathbf{u}_{p+2}, \cdots, \mathbf{u}_M] \\ \mathbf{\Lambda}_n &= \mathrm{diag}(\lambda_{p+1}, \lambda_{p+2}, \cdots, \lambda_M) \end{aligned} . \tag{5}$$

In practical applications, $\mathbf{R}_{main}(f_j)$ can be replaced by the covariance matrix $\hat{\mathbf{R}}_{main}(f_j)$ of the actual received signal as

$$\hat{\mathbf{R}}_{main}(f_j) = \frac{1}{K} \sum_{k=1}^{K} \mathbf{X}_{main}(f_j) \mathbf{X}_{main}^H(f_j) \tag{6}$$

In (6), K denotes the number of training snapshots. Various jammings and noises can be distinguished using eigenvalues, with each corresponding to a specific eigenvector. This one-to-one correspondence allows for the determination of signals associated with the obtained eigenvectors. Consequently, the correlation coefficient method is utilized to identify the eigenvectors representing main lobe jamming within the eigenvector space. Following this identification, a blocking matrix is derived for preprocessing, aimed at effectively filtering out main lobe jamming components from the received data.

The blocking matrix $\mathbf{B}(f_j)$ for the jth sub-channel can be given by (7) as

$$\mathbf{B}(f_j) = \mathbf{I} - \mathbf{u}_m (\mathbf{u}_m^H \mathbf{u}_m)^{-1} \mathbf{u}_m^H \tag{7}$$

where $\mathbf{I}$ is the identity matrix of $M \times M$. The eigenvector u_m, corresponding to the main lobe jamming, can be obtained as

$$\left|\rho(\mathbf{u}_m, \mathbf{a}(\theta_0, f_j))\right| = \max_{\mathbf{u}_i} \left|\rho(\mathbf{u}_i, \mathbf{a}(\theta_0, f_j))\right| \tag{8}$$

where $\rho(\mathbf{a}_1, \mathbf{a}_2)$ denotes the correlation coefficient of vectors $\mathbf{a}_1$ and $\mathbf{a}_2$, which is defined as

$$\rho(\mathbf{a}_1, \mathbf{a}_2) \triangleq \frac{\mathbf{a}_1^H \mathbf{a}_2}{\|\mathbf{a}_1\| \|\mathbf{a}_2\|} \tag{9}$$

The conventional eigenprojection matrix is not capable of fully eliminating the influence of the main lobe jamming, which may result in a bias in the estimation of the side lobe jamming. In order to completely remove the main lobe jamming component, the jamming plus noise covariance matrix is reconstructed by nullifying the main lobe jamming power. Furthermore, zero-constraint beamforming is performed to accurately suppress the side lobe jamming. The reconstructed covariance matrix is expressed as

$$\mathbf{R}_{main\_re}(f_i) = \mathbf{V}(f_j)\mathbf{P}\mathbf{V}^H(f_j) + \hat{\sigma}_n^2 \mathbf{I} \tag{10}$$

where $\mathbf{V}(f_j)$ represents the matrix composed of corrected signal steering vectors, $\mathbf{P}$ denotes the reconstructed estimated power diagonal matrix, and $\hat{\sigma}_n^2 \mathbf{I}$ signifies the estimated noise power. They can be calculated as

$$\begin{aligned} \hat{\sigma}_n^2 &= \frac{\sum_{i=p+1}^{M} \lambda_i}{M-p} \\ \mathbf{P} &= diag(0, \delta_{j1}, \cdots, \delta_{ji}, \cdots, \delta_{j(p-1)}) \\ \mathbf{V}(f_j) &= [\mathbf{u}_m, \mathbf{B}(f_j)\mathbf{u}_{j1}, \cdots, \mathbf{B}(f_j)\mathbf{u}_{ji}, \cdots, \mathbf{B}(f_j)\mathbf{u}_{j(p-1)}] \end{aligned} \tag{11}$$

where $\mathbf{u}_{ji}$ represents the side lobe jamming eigenvector in the jamming subspace, and δ_{ji} is the corresponding power estimate calculated as

$$\delta_{ji} \approx \frac{\lambda_{ji} - \hat{\sigma}_n^2}{M} \tag{12}$$

This reconstruction method can still achieve effective beamforming performance when the training data include the desired signal. By zeroing out the power of the main lobe jamming, it completely removes the main lobe jamming component, avoiding deviation of the main beam and does not affect the formation of nulls at the sidelobe jamming locations.

The angle of the side lobe jamming is determined through spatial spectrum estimation, which is then used to inform zero-constraint beamforming. The spatial spectrum of the main array is depicted in Figure 3. It can be observed that the side lobe jamming originates at the angle of 20°.

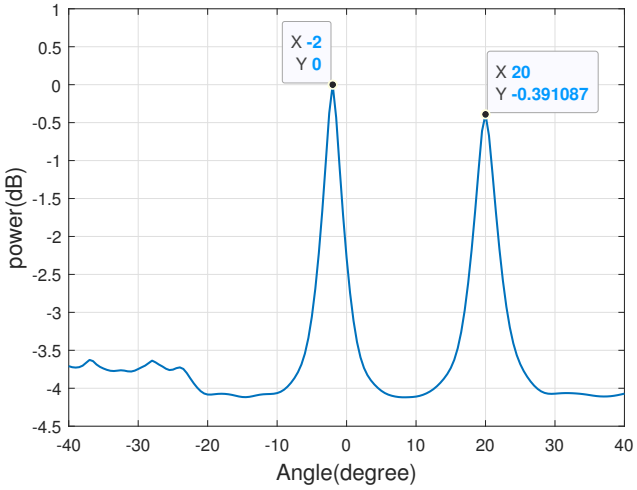

Figure 3. Spatial spectrum of full array.

The final adaptive weight vector for the jth subband is obtained as:

$$\mathbf{w}_{main}(f_j) = \frac{\mathbf{R}^{-1}_{main\_re}(f_j)\mathbf{C}(f_j)}{\mathbf{C}^H(f_j)\mathbf{R}^{-1}_{main\_re}(f_j)\mathbf{C}(f_j)}\mathbf{f} \tag{13}$$

where $\mathbf{C}(f_j) = [\mathbf{a}(\theta_0, f_j), \mathbf{a}(\theta_{j1}, f_j), \cdots, \mathbf{a}(\theta_{j(p-1)}, f_j)]$, $\mathbf{f} = [1, 0, \cdots, 0]$.

The effect of the eigenvalues of the main lobe jamming is negated when the covariance matrix is derived, thus enabling the beam pattern main array to accurately align the null-trapping with the side lobe jamming while maintaining the main lobe. The final frequency domain output of the main array is

$$\mathbf{Y}_{main} = \left[\mathbf{w}^H_{main}(f_1)\mathbf{X}_{main}(f_1), \cdots, \mathbf{w}^H_{main}(f_J)\mathbf{X}_{main}(f_J)\right] \tag{14}$$

To implement the joint beamforming technique described later, it is crucial to direct a narrow beam toward the main lobe jamming within the full array using sub-band adaptive beamforming (SAB). The narrowness of the auxiliary beam enables the main array beam to form a narrow null-trapping at the main lobe jamming, thus allowing both main and side lobe jamming to be effectively suppressed in the final output, while reducing signal loss. The main lobe jamming incidence angle can be identified from the spatial spectrum of the main array. Provided that the aperture of the full array is sufficiently large, the beam directed at the main lobe jamming can be highly focused. The frequency domain output of the full array is $\mathbf{Y}_{full}$.

3.2. Joint Beamforming Using MMSE

For the purpose of joint beamforming, the time–domain outputs of the two arrays are crucial, which can be obtained using fast Fourier transform as

$$\begin{aligned} \mathbf{y}_{main}(t) &= IFFT[\mathbf{Y}_{main}] \\ \mathbf{y}_{full}(t) &= IFFT\left[\mathbf{Y}_{full}\right] \end{aligned} \tag{15}$$

The output of the full array is used as an auxiliary signal and weighted, and then the weighted signal is subtracted from the output of the main array to obtain the final signal that successfully eliminates the jamming of the main and side lobe.

$$\mathbf{y}(t) = \mathbf{y}_{main}(t) - \mathbf{w}^H_{MMSE}\mathbf{y}_{full}(t) \tag{16}$$

where $\mathbf{w}_{MMSE}$ is weight vector calculated by the MMSE,

$$\mathbf{w}_{MMSE} = \mathbf{R}^{-1}r \tag{17}$$

where $\mathbf{R} = E\left\{\mathbf{y}_{full}(t)\mathbf{y}^H_{full}(t)\right\}$, $r = E\left\{\mathbf{y}_{full}(t)\mathbf{y}^*_{main}(t)\right\}$.

Traditional single radar main lobe jamming suppression methods create a wide null in the main lobe jamming area, which can affect the reception of desired signals. In contrast, the joint beamforming method utilizes a sufficiently large auxiliary array to form a narrower beam. By subtracting the weighted narrow beam from the main array's output, a narrower null can be achieved in the main lobe jamming area, thereby reducing the impact on the reception of desired signals while maintaining effective main lobe jamming suppression.

4. Simulations

To validate the efficacy of the algorithm, we conduct simulations in this chapter. We consider a distributed array comprising 12 uniform linear arrays (ULAs). Additionally, we randomize the distances between the ULAs to mitigate grating lobes outside the main lobe and nulls within it. The other simulation conditions are as follows. The number of main array elements M of ULA is 20, and the spacing between array elements is half-wavelength corresponding to the highest frequency of the working band. The lowest frequency of the simulated signal is 0.7 GHz , the highest frequency is 1 GHz. The desired signal is incident

from the direction of $-5°$, and the noise is Gaussian white noise with a signal-to-noise ratio (SNR) of 0 dB. There are two jamming signals, one is the main lobe jamming, and the other is the side lobe jamming. The main lobe jamming comes from the direction of $-2°$ with a interference-to-noise ratio (INR) of 40 dB. The side lobe jamming comes from the direction of $20°$ with INR of 40 dB. The signals received by the array are divided into signal bands through DFT, with the number of sub-bands set to 128, and the number of snapshots set to 1024.

4.1. Performance Simulation under Different Array Aperture

With uniform element spacing, we adjust the array aperture by varying the number of elements. Consider an auxiliary array with 12 elements, which has a smaller aperture compared to the main array. In this scenario, the beam patterns at various stages of different arrays are shown in Figure 4.

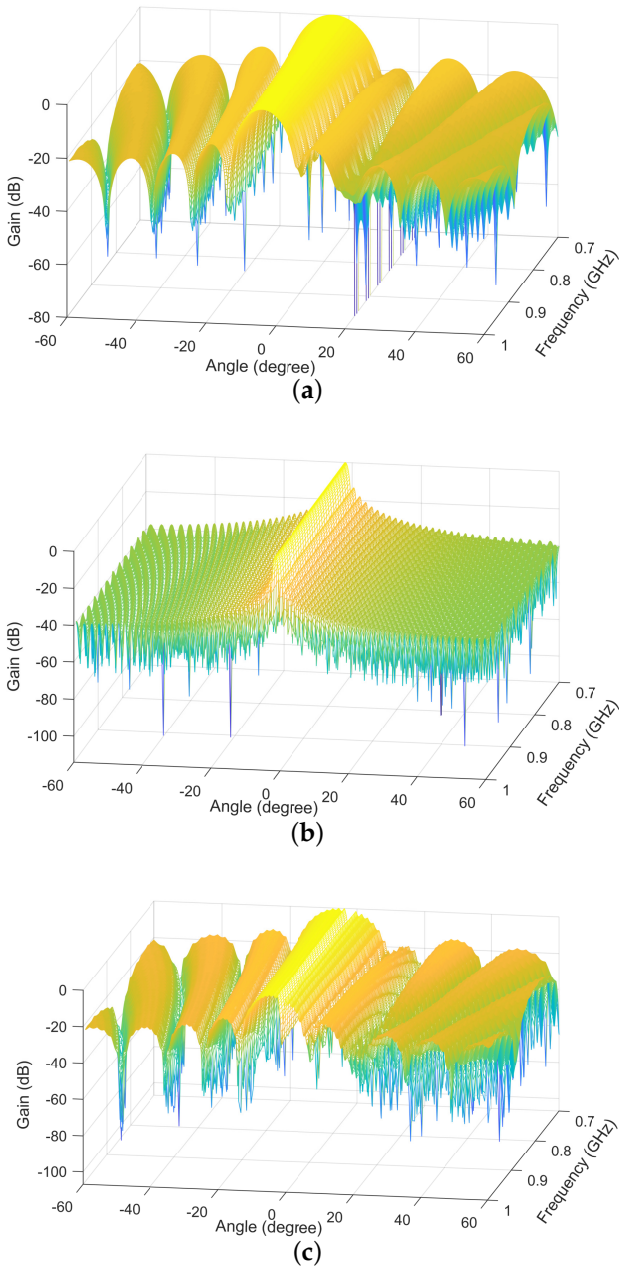

Figure 4. Beam patterns under different array aperture. (**a**) Main array, (**b**) full array, (**c**) joint beamforming.

Traditional methods for suppressing main lobe jamming suffer from a wide null along the main lobe jamming, which can lead to distortion and peak shifting of the main lobe. In contrast, the proposed joint beamforming method forms separate beams targeting the desired signal and main lobe interference, effectively mitigating the impact of main lobe jamming on the desired signal. Simultaneously, this joint beamforming approach subtracts a weighted narrow beam from the main channel, resulting in a narrower null at the main lobe jamming. With a sufficiently large auxiliary array aperture, the null caused by main lobe jamming can be controlled within a certain range, thereby minimizing its impact on the beam's main lobe to the greatest extent possible.

4.2. Performance Simulation under Same Array Aperture

The method proposed in this paper theoretically demonstrates better performance when the array has a large aperture size. Therefore, this section will present and discuss performance simulation and analysis under the condition of the same aperture for the main and auxiliary arrays.

Figure 5 shows the beam patterns at various stages of the proposed method under the same array aperture. From Figure 5a, it can be observed that the main array forms nulls at the angles of side lobe jamming, while the main lobe remains undisturbed. The full array forms a pattern with high gain at the main lobe jamming angle in Figure 5b. In Figure 5c, the beam pattern diagram after joint beamforming using MMSE exhibits nulls at the angles of both main lobe jamming and side lobe jamming, while achieving a relatively complete preservation of the main lobe. Compared to traditional SAB methods, this approach can accurately suppress jamming with minimal impact on the desired signal and main lobe.

Figure 6 shows the variation of output signal-to-interference-plus-noise ratio (SINR) with respect to input SNR. Under identical conditions, the proposed algorithm clearly outperforms the conventional SAB algorithm of individual arrays in terms of output SINR.

The variation in output signal-to-interference-plus-noise ratio (SINR) with respect to snapshots is shown in Figure 7. It can be observed that the algorithm proposed herein exhibits a convergence speed similar to conventional SAB methods. However, due to its superior maintenance of the main lobe, which reduces signal loss, the proposed algorithm achieves higher SINR output compared to conventional SAB.

Figure 8 provides a further analysis of the specific impact of the proposed algorithm on target detection through the quantitative evaluation of SINR loss. Given all other conditions remain unchanged, if the desired signal enters from within the main lobe at an angle θ, the signal loss can be defined as

$$SINR_{loss} = \frac{\hat{P}_{s(\theta)} \Big/ \left(\hat{P}_i + \hat{P}_{noise}\right)}{P_{s(\theta)} \Big/ P_{noise}} \tag{18}$$

where $\hat{P}$ denotes the output signal power of the beam formation, and P denotes the output signal power without the beam formation. It is clear that only when the deviation between the main lobe jamming angle and the desired signal angle is small, the SINR loss is significant. In other main lobe regions, the SINR loss is acceptably small.

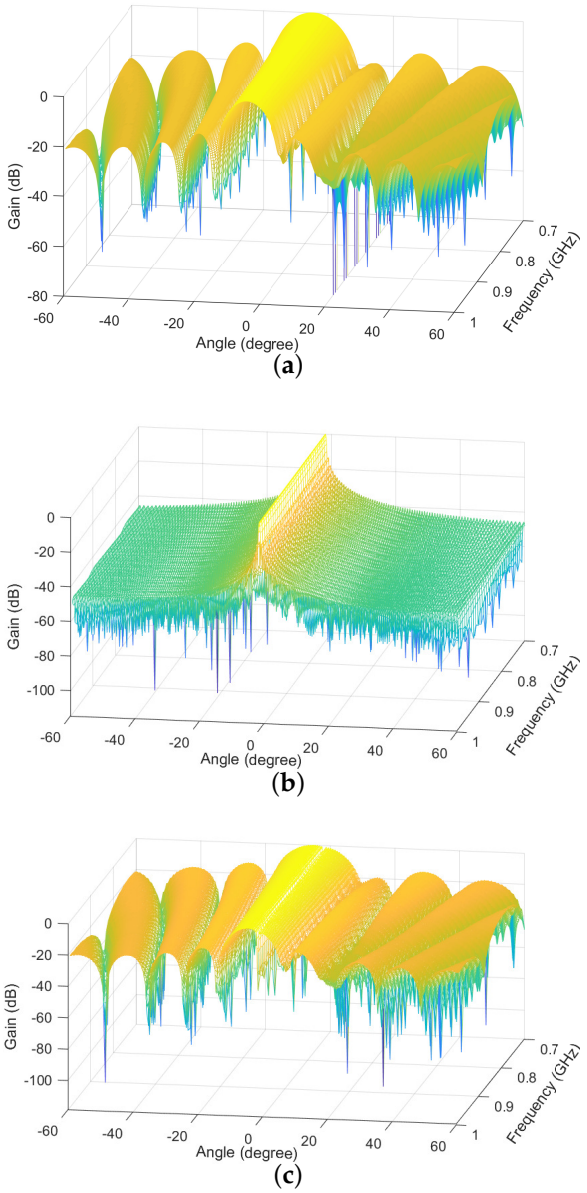

Figure 5. Beam patterns under same array aperture. (**a**) Main array, (**b**) full array, (**c**) joint beamforming.

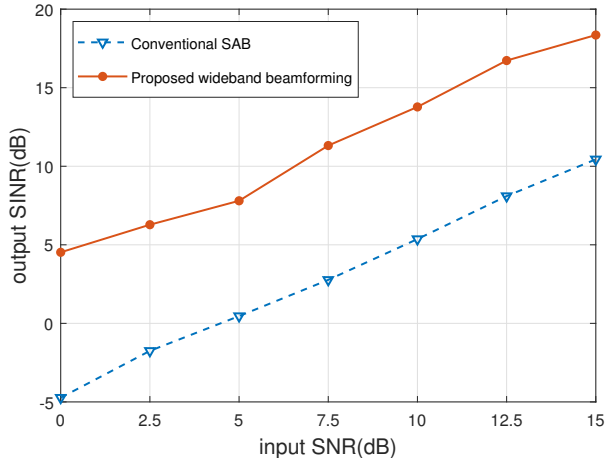

Figure 6. Output SINR versus input SNR.

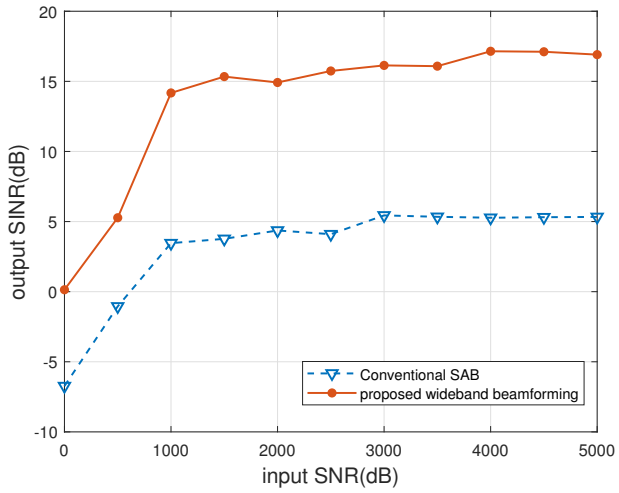

Figure 7. Output SINR versus snapshots.

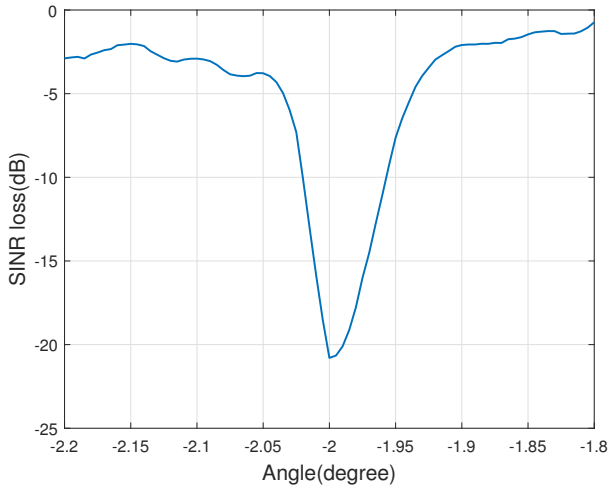

Figure 8. SINR loss by adaptive beamforming.

5. Conclusions

A wideband main lobe jamming suppression method based on distributed array radar is proposed in this paper. This method applies the EMP algorithm and null constraint beamforming in the main array to achieve sidelobe jamming suppression while maintaining the integrity of the main lobe. In the full array, a narrow beam directed at the main lobe jamming is formed. Finally, by combining the beamforming outputs of the two arrays, joint beamforming using the MMSE criterion suppressed the main lobe jamming. Jamming cancellation performance verified the correctness and simulation results. However, it is important to note a limitation of our approach: it relies on high accuracy in spatial spectral estimation. Achieving this level of precision may pose challenges in practical scenarios. Addressing this limitation could be a focus for future research efforts.

Author Contributions: Writing—original draft preparation, X.M.; investigation, X.M. and S.J.; writing—review and editing, S.J. and S.Z.; project administration, S.Z., X.M., S.J. and R.Z.; supervision, W.S.; funding acquisition, S.Z. and R.Z. All authors have read and agreed to the published version of the manuscript.

Funding: This work was supported in part by the National Natural Science Foundation of China under Grant 62001227 and Grant 62371236, and by the Graduate Research and Practice Innovation Program of Jiangsu Province under Grant SJCX24_0144.

Institutional Review Board Statement: Not applicable.

Informed Consent Statement: Not applicable.

Data Availability Statement: Not applicable.

Acknowledgments: The authors thank the reviewers for their great help on the article during its review progress.

Conflicts of Interest: The authors declare no conflicts of interest.

References

1. Li, K.; Jiu, B.; Liu, H.; Pu, W. Robust Antijamming Strategy Design for Frequency-Agile Radar against Main Lobe Jamming. *Remote Sens.* **2021**, *13*, 3043. [CrossRef]
2. Pan, B.; Dong, L.; Yu, X.; Yao, X.; Sha, M.; Cui, G. Joint Polarization-Space-Time Processing for Mainlobe Jamming via CP Decomposition. *IEEE Sens. J.* **2023**, *23*, 14781–14794. [CrossRef]
3. Chen, J.; Chen, X.; Zhang, H.; Zhang, K.; Liu, Q. Suppression Method for Main-Lobe Interrupted Sampling Repeater Jamming in Distributed Radar. *IEEE Access* **2020**, *8*, 139255–139265. [CrossRef]
4. Zhang, Y.; Liao, G.; Xu, J.; Zhang, X.; Lan, L. A Method to Suppress Interferences Based on Secondary Compensation with QPC-FDA-MIMO Radar. *Remote Sens.* **2023**, *15*, 4711. [CrossRef]
5. Tian, D.; Wang, C.; Ren, W.; Liang, Z.; Liu, Q. ECCM Scheme for Countering Main-Lobe Interrupted Sampling Repeater Jamming via Signal Reconstruction and Mismatched Filtering. *IEEE Sens. J.* **2023**, *23*, 13261–13271. [CrossRef]
6. Wang, H.; Zhang, Z.; Li, Y.; Feng, Z. Improved Main-Beam Nulling through Single Switchable Displaced Element for Small Scale Adaptive Array. *IEEE Trans. Antennas Propag.* **2014**, *62*, 2522–2530. [CrossRef]
7. Godara, L. Application of antenna arrays to mobile communications. II. Beam-forming and direction-of-arrival considerations. *Proc. IEEE* **1997**, *85*, 1195–1245. [CrossRef]
8. Jin, G.; Wang, Y.; Zhu, D.; Niu, S.; Yan, H. A Reconfigurable MIMO-SAR Transmission Scheme Based on Inter-Pulse and Intra-Pulse Joint Phase Modulation. *IEEE Trans. Signal Process.* **2022**, *70*, 4265–4276. [CrossRef]
9. Nanzer, J.A.; Mghabghab, S.R.; Ellison, S.M.; Schlegel, A. Distributed Phased Arrays: Challenges and Recent Advances. *IEEE Trans. Microw. Theory Tech.* **2021**, *69*, 4893–4907. [CrossRef]
10. Haimovich, A.M.; Blum, R.S.; Cimini, L.J. MIMO Radar with Widely Separated Antennas. *IEEE Signal Process. Mag.* **2008**, *25*, 116–129. [CrossRef]
11. Ganz, M.; Ward, J.; Carlson, B. Mainbeam nulling with adaptive array interferometry. In Proceedings of the Conference Record of the Twenty-Fifth Asilomar Conference on Signals, Systems & Computers, Pacific Grove, CA, USA, 4–6 November 1991; Volume 2, pp. 974–978. [CrossRef]
12. Yang, X.; Yin, P.; Zeng, T.; Sarkar, T.K. Applying Auxiliary Array to Suppress Mainlobe Interference for Ground-Based Radar. *IEEE Antennas Wirel. Propag. Lett.* **2013**, *12*, 433–436. [CrossRef]
13. Zhang, H.; Luo, J.; Chen, X.; Liu, Q.; Zeng, T. Whitening Filter for Mainlobe Interference Suppression in Distributed Array Radar. In Proceedings of the 2016 CIE International Conference on Radar (RADAR), Guangzhou, China, 10–13 October 2016; pp. 1–5. [CrossRef]
14. Liu, R.; Zhang, W.; Yu, X.; Lu, Q.; Wei, W.; Kong, L.; Cui, G. Transmit-Receive Beamforming for Distributed Phased-MIMO Radar System. *IEEE Trans. Veh. Technol.* **2022**, *71*, 1439–1453. [CrossRef]
15. Chen, X.; Shu, T.; Yu, K.B.; Zhang, Y.; Lei, Z.; He, J.; Yu, W. Implementation of an Adaptive Wideband Digital Array Radar Processor Using Subbanding for Enhanced Jamming Cancellation. *IEEE Trans. Aerosp. Electron. Syst.* **2021**, *57*, 762–775. [CrossRef]
16. Chen, X.; Shu, T.; Yu, K.B.; He, J.; Yu, W. Joint Adaptive Beamforming Techniques for Distributed Array Radars in Multiple Mainlobe and Sidelobe Jammings. *IEEE Antennas Wirel. Propag. Lett.* **2020**, *19*, 248–252. [CrossRef]
17. Han, B.; Yang, X.; Lv, Q.; Li, W.; Zhang, Z.; Zhong, S. Mainlobe and sidelobe jamming suppression method based on distributed array radar with eigen-projection matrix processing and null constraints. *IET Radar Sonar Navig.* 2024, *early view*. [CrossRef]
18. Pu, W.; Liang, Z.; Wu, J.; Liu, Q. Joint Generalized Inner Product Method for Main Lobe Jamming Suppression in Distributed Array Radar. *IEEE Trans. Aerosp. Electron. Syst.* **2023**, *59*, 6940–6953. [CrossRef]